International Journal of Impact Engineering 143 (2020) 103597

Contents lists available at ScienceDirect

International Journal of Impact Engineering

journal homepage: www.elsevier.com/locate/ijimpeng

Experimental and numerical analysis of PMMA impact fracture

N.A. Kazarinov[a,*], V.A. Bratov[a,b], N.F. Morozov[a,b], Y.V. Petrov[a,b], V.V. Balandin[c], M.A. Iqbal[d], N.K. Gupta[e]

[a] Department of Theory of Elasticity, Saint Petersburg State University, Saint Petersburg, Russia
[b] Institute of Problems of Mechanical Engineering, Russian Academy of Sciences, Saint Petersburg, Russia
[c] Institute of Mechanics, Lobachevsky State University of Nizhni Novgorod, Nizhni Novgorod, Russia
[d] Department of Civil Engineering, Indian Institute of Technology Roorkee, Roorkee, India
[e] Department of Applied Mechanics, Indian Institute of Technology Delhi, Hauz Khas, New Delhi, India

ARTICLE INFO

Keywords:
Impact
Penetration
PMMA
Threshold velocity
FEM
Incubation time

ABSTRACT

The work presents experimental and numerical results on dynamic fracture of PMMA plates subjected to impact loading. The experimental tests were conducted using steel cylinder-shaped projectile accelerated using a gas gun. In order to evaluate performance of the tested specimens, residual impactor velocity was assessed using high-speed photography setup. Square-shaped PMMA specimens with three thicknesses were investigated using various projectile velocities. For all the three specimen types the ballistic limits were experimentally obtained. The conducted experiments were numerically simulated using finite element method with explicit time integration scheme and incubation time fracture model for the material failure prediction. Experiments with all three specimen configurations were successfully simulated using one parameter – incubation time, which was evaluated from existing experimental data on the dynamic fracture of PMMA. In addition to the simulations of the real experiments estimates on performance of a sample with a virtual geometry were made using the developed numerical approach.

1. Introduction

Impact fracture of materials is of high importance for engineering applications, since this phenomenon is ubiquitous: design of military protective systems, (bulletproof vests, vehicle armor, etc.), automotive industry (car crash safety), aeronautics (bird impacts, space debris threat, solid particle erosion of turbine blades), electronics (drops of handheld devices), etc. Experiments on impact fracture of materials are time and effort-consuming, since they require high-speed registering systems and precise synchronization of the equipment. Moreover, these experiments can be rather costly, since specimens are disposable. Numerical simulations can serve as a tool to optimize experimental studies and the product design due to constantly increasing computational capabilities of contemporary machines. A wide variety of numerical approaches to the dynamic fracture problems are now presented in the literature, which include finite element method with cohesive zones approach (e.g. see classic works by Needleman [1]), smooth particle hydrodynamics methods [2,3], discrete particle approach [4] Element-free Galerkin methods [5], perydynamics [6,7]. However, apart from the numerical scheme choice an appropriate fracture model should be applied since materials can exhibit complicated behavior when subjected to intensive dynamic loading: increasing strength with a growing strain rate [8,9], peculiarities related to dynamic crack propagation [10,11], problems of dynamic fragmentation of solids [12].

According to one of the most common approaches to the dynamic fracture modeling strain rate dependencies are explicitly introduced into the material models. Johnson-Cook constitutive model [13, 14] is a prominent representative of this approach being one of the most used material models in the field of impact engineering and dynamic fracture. This model has been successfully applied in a vast number of works, however, it contains a relatively large set of parameters to be defined using rather complicated procedures [15,16] and not all of these parameters have a clear physical interpretation. Analogous approach is used to predict the dynamic fracture in specimens with cracks: classic fracture criterion by Irwin [17] is extended to the dynamic case by introduction of the strain rate dependencies and substitution of the material parameters by functionals [18, 19]. These functional dependencies are regarded as material properties that should be evaluated experimentally. In general, the strain rate-dependent fracture models rely on comparatively large sets of parameters and functional dependencies, which are sometimes hard to evaluate experimentally.

* Corresponding author.
E-mail address: n.kazarinov@spbu.ru (N.A. Kazarinov).

https://doi.org/10.1016/j.ijimpeng.2020.103597
Received 5 August 2019; Received in revised form 15 April 2020; Accepted 15 April 2020
Available online 06 May 2020

A relatively effective approach to the engineering problems is based on the introduction of dimensionless damage numbers [20, 21], which describe behavior of the structure subjected to dynamic loading. These numbers are evaluated using parameters characterizing loading, geometry of samples and material mechanical properties. The damage numbers provide possibility to estimate structure response to dynamic loading and to compare the structure performance for various testing conditions (target shape and dimensions, loading parameters, material parameters).

Another group of the dynamic fracture criteria are based on time characteristics of the fracture process. In this work incubation time fracture model [22,23,24] was used to perform numerical simulations of impact experiments on PMMA conducted within the study. Impactor velocity drop due to interaction with the target was registered in these tests. The experiments were conducted on specimens with three thicknesses and the incubation time model which includes a single time parameter was able to provide good agreement between experiments and numerical simulations for all three sample geometries and a wide range of the impactor velocities. The incubation time value for the PMMA had been evaluated in previous works using experiments on spallation in rods due to impact. Different time-based integral models have been recently successfully applied to simulate impact damage [25], however the approach used in the presented work relies on the incubation time parameter which is considered to be a material property and can be assessed from experiments.

The PMMA was used since it can be regarded as a benchmark material for the dynamic fracture research. This material exhibits remarkable properties which are valuable for the fundamental fracture studies: it is transparent and birefringent and thus methods of caustics and fringe patterns stress analysis are applicable, moreover PMMA can be regarded as a brittle material. This material has been used in numerous works on dynamic crack propagation [26, 27], impact [25, 28], spallation [29, 30] and its strength parameters and behavior are well-known. On the other hand, the PMMA is widely used for various engineering applications [31] and the results of this work (both experimental and numerical) can be useful for practical needs.

2. Experimental tests

Square (100mm x 100mm) PMMA plates with three thicknesses (4 mm, 6 mm and 10 mm) were studied. The sample was clamped in a four-arm holder (see Fig. 1)

In order to conduct impact tests a gas gun experimental facility was used. The setup is schematically shown in Fig. 2. The initial projectile velocity was controlled by air pressure in the system and appropriate choice of the membranes placed in the gun shatter. Two membranes were used in the shatter and each could sustain half of the operating pressure. Due to pressure drop in the auxiliary pressure chamber the membranes broke and the projectile started to move through the barrel. The initial velocity was measured using a magnetic coil placed at the exit end of the barrel, while the residual impactor velocity was evaluated using HSFC pro high-speed photography equipment, produced by PCO AG. This setup consists of four Dicam pro modules, which provide possibility to capture eight frames with a variable time interval. For almost all the experiments 150 μs inter-frame time interval.

Fig. 1. The sample mounting device: four grips fixing the specimen (fitting: single).

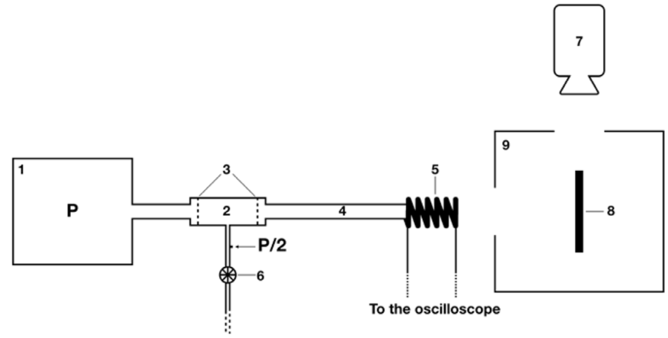

Fig. 2. Scheme of the experimental setup; 1 – high pressure chamber, 2 – shatter device, 3 – membranes, 4 – barrel, 5 magnetic coil for the impactor velocity measurements, 6 – pressure drop valve to trigger a shot, 7 – high-speed camera rig, 8 – sample, 9 – protection chamber; P indicates pressure (fitting: 1.5).

Steel cylindrical impactor (diameter 6 mm, length 20 mm and mass 8.3 grams) was accelerated to velocities ranging from 40 m/s to 350 m/s. The impactor was placed in a disposable aluminum bed which fitted precisely the gun barrel. The bed was stopped by a barrier at the end of the barrel and the impactor continued to move leaving the bed. The contact between the bed and the barrier caused linkage of the electrical circuit and enabled triggering the high-speed photography setup with a programmable time delay.

3. Numerical scheme

3.1. Incubation time fracture model

The incubation time fracture criterion was originally proposed by Petrov and Utkin in [22]. The incubation time approach regards macroscopic experimentally observable fracture as a non-instantaneous event, which requires a specific time to develop. The macroscopic fracture results from microscopic preparatory processes such as microcracking, interaction of pores and defects etc. The time taken by these preparatory processes is considered to be a material property to be assessed experimentally. This parameter is called the incubation time and the corresponding microscopic fracture processes are often referred to as the incubation processes.

According to the model the fracture initiation condition reads as:

$$\frac{1}{\tau}\int_{t-\tau}^{t}\frac{1}{d}\int_{x-d}^{x}\sigma(x', t')dx'dt' \geq \sigma_c, \tag{1}$$

where $\sigma(x, t)$ is a time-dependent stress at point x, σ_c is the material static ultimate tensile stress and τ stands for the incubation time.

The criterion (1) contains linear size parameter d, which was firstly introduced as a fracture process parameter by Neuber [32] and Novozhilov [33] for static problems with a complex geometry. This parameter is treated as the minimal characteristic size of the fractured material volume. This way, fracture is a spatially non-local phenomenon with a step-like development, since fracture occurs in a d-sized

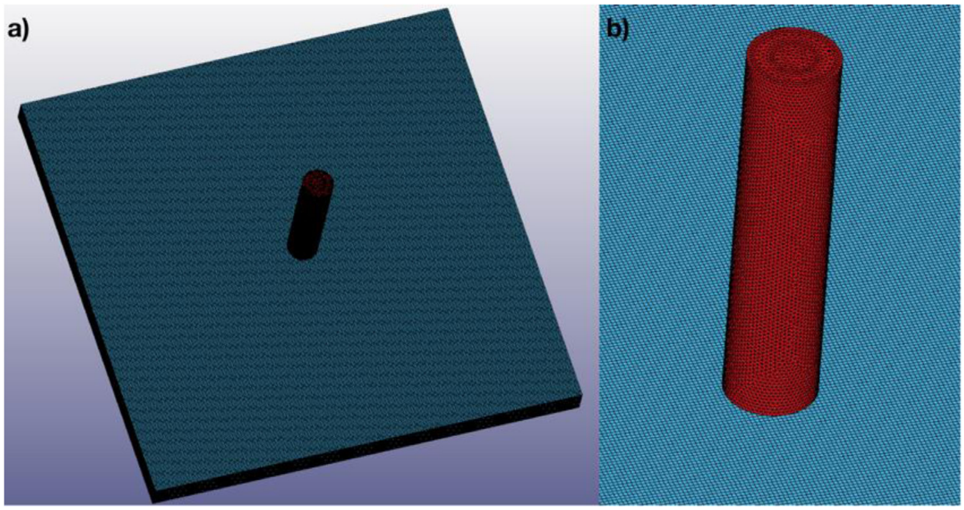

Fig. 3. Finite element mesh with an enlarged contact area (b). The model for a 6 mm plate is shown (fitting: single).

Table 1
Material properties used in the numerical model.

	PMMA target	Steel projectile
Young's modulus, E, Pa	3.3e9	2.09e11
Poisson's ratio, ν	0.35	0.28
Density, ρ, kg/m^3	1180	7720
Ultimate tensile stress, σ_c, Pa	72e6	-
Ultimate stress intensity factor, K_{Ic}, MPa	1.7	-
Incubation time, τ, μs	1	-

domain containing point x. This approach fits perfectly into the framework of numerical simulations, as numerical solutions of the solid mechanics equations usually imply spatial discretization of the modeled bodies. The linear size d can be calculated using expression $d = 2K_{Ic}^2/\pi\sigma_c^2$, where K_{Ic} is the critical stress intensity factor (mode I loading is supposed) for the studied material.

The left side of inequality (1) contains integration over time and thus history of the stresses is accounted for. The microscopic fracture processes are supposed to develop due to these stresses and specific time τ is needed for the macroscopic fracture to evolve.

The criterion (1) can be reformulated for the case of the dynamic crack initiation problem using linear fracture mechanics methods:

$$\frac{1}{\tau}\int_{t-\tau}^{t} K_I(t')dt' \geq K_{Ic}, \tag{2}$$

where $K_I(t)$ is a time-dependent stress intensity factor for a mode I loading.

The incubation time parameter τ can be evaluated from experiments on dynamic fracture. In order to calculate the incubation time value, one should register fracture initiation time and the stress – time dependence in the point of interest. The stress – time function is then substituted to formula (1) and τ is evaluated as a fitting parameter so that fracture occurs at the registered fracture initiation time. Experiments on spallation or dynamic crack initiation can be used to obtain the incubation time value. It should be noted here that an adequate choice of the fracture scale level is crucial for the sake of the simulation correctness. One should define fracture scale level to be considered in the studied problem and then use an appropriate τ value, which was measured on an appropriate scale level. For a more detailed discussion on the fracture scales please refer to the work presented in [34].

3.2. Finite element model

The developed numerical scheme is based on a finite element method with explicit time integration and LS-DYNA software is used as a solver. The incubation time fracture criterion was implemented via user defined material (UMAT41 routine) in the LS-DYNA code. Evolution of stresses for each element is stored in additional array parameter and time integral in the inequality (1) is computed according to the trapezoidal integration rule. The element size equals linear size d used in the incubation time fracture condition (1) and element deletion technique is implemented in order to simulate the fracture development. This scheme fits perfectly the incubation time approach since the

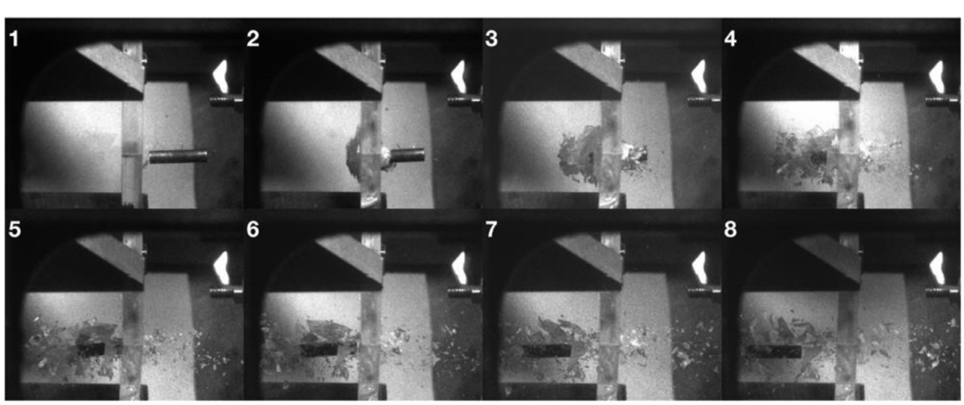

Fig. 4. The speed-photography frame sequence used to calculate the impactor residual velocity. 10 mm thick target and 144 m/s initial impactor velocity case depicted (fitting double).

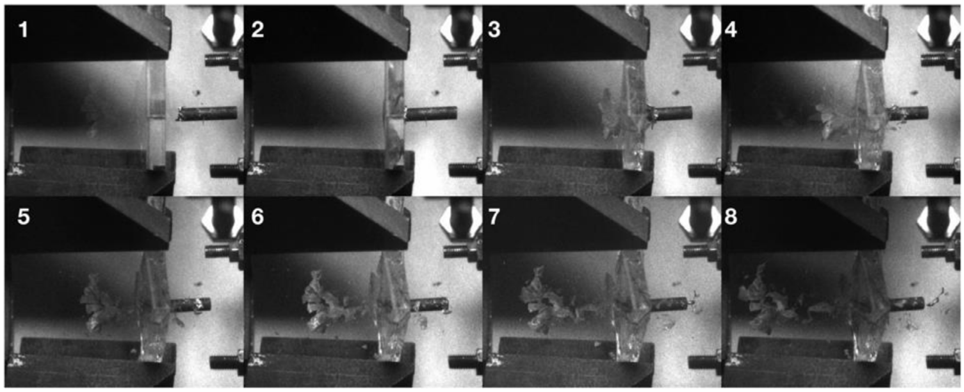

Fig. 5. High-speed photography of the threshold velocity impact: 10 mm plate thickness and 70 m/s impactor velocity (fitting double).

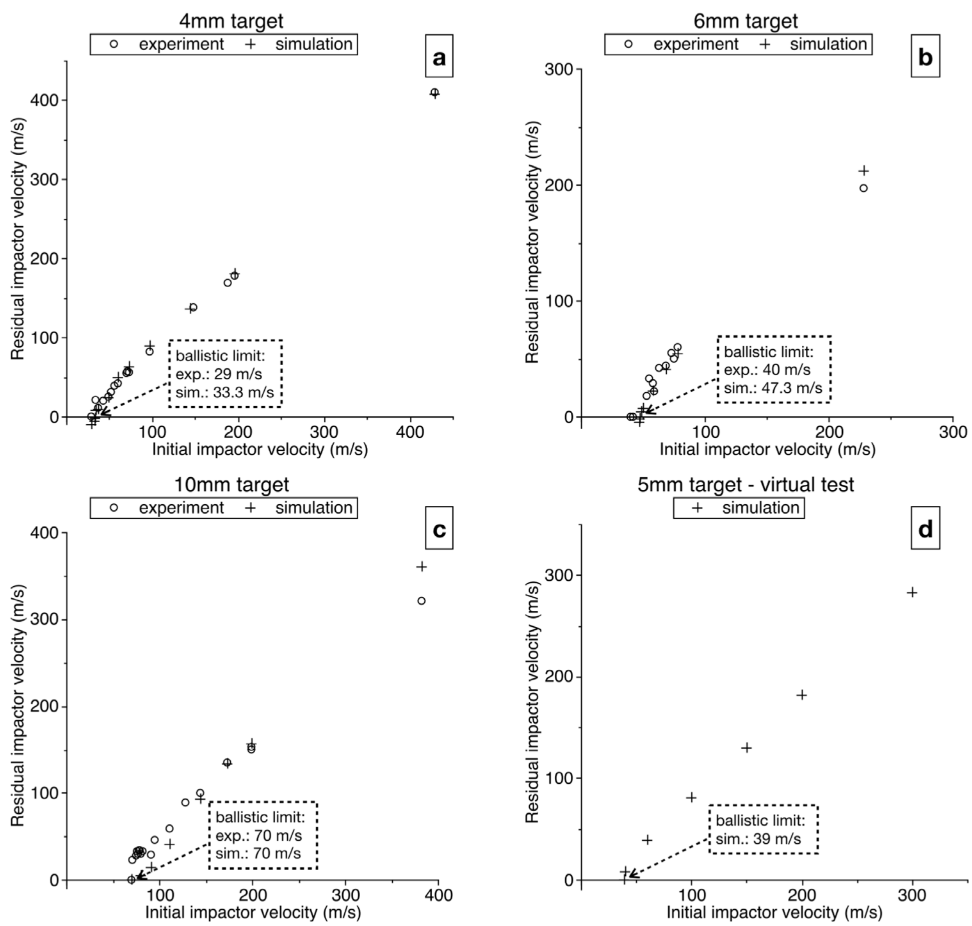

Fig. 6. Residual velocity – initial velocity dependencies for different specimen thicknesses; (a)–(c) comparison of the experimental and numerical data (d) a mere numerical prediction and the arrows indicate the ballistic limit (fitting: double).

minimal characteristic size of a fractured region equals *d*. Mesh sensitivity testing revealed that further reduction of the element size does not affect the computation results.

A fully integrated (with 8 integration points) solid element was found to be the most robust in terms of stability of the numerical simulation. The finite element mesh is shown in Fig. 3. The problem is solved in a three-dimensional statement and the boundary conditions are satisfied due to displacement restrictions imposed on the nodes lying under the holder grips (see Fig. 1).

The material parameters used in the simulations are listed in Table 1. All the properties were either taken from the material information sheet supplied by the PMMA manufacturer or from elsewhere [35]. The material behavior was supposed to be governed by Hooke's law and thus two material parameters (Young's modulus and Poisson's ratio) were sufficient for the stress-strain dependency description. The incubation of 1 μs provided a good coincidence between the numerical results and the experimental data. This value is close to the PMMA incubation time for a “small” scale level (0.8 μs) calculated in [34]. According to [34] the 0.8 μs value was obtained from experiments on spallation of PMMA rods, where microcracking (small-scale fracture) was registered. Element erosion applied in our scheme can be also considered as a small-scale fracture since the element size is small comparing to the sample dimensions.

This way, application of a 1 μs incubation time is correct within the

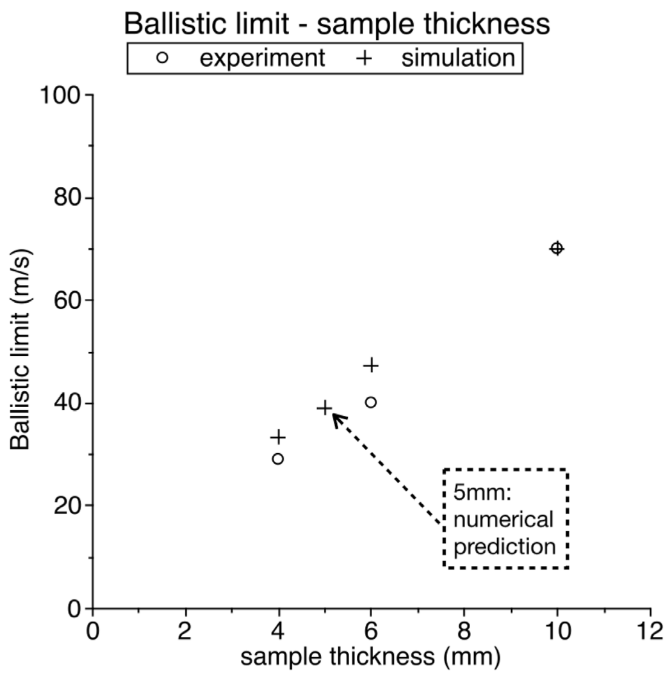

Fig. 7. Ballistic limit – sample thickness dependence; 5 mm point is a numerical prediction (fitting: single).

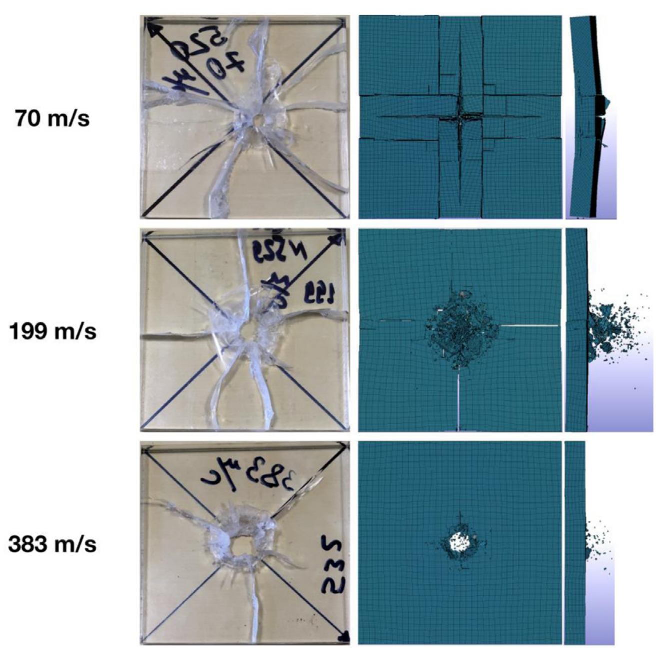

Fig. 8. Fracture patterns: experiment and numerical simulation; 10 mm plate results are shown (fitting: 1.5).

studied case. The incubation time values close to 1 μs have been also used to simulate dynamic crack propagation in PMMA specimens [27,36].

The element size selection resulted in a fine finite element mesh: the regular mesh for the thickest target (10 mm) contains 2306196 solid elements, while the impactor consists of 26745 solid elements.

4. Results

Here we provide both experimentally obtained data and results of numerical simulations using the developed scheme. Fig. 4 shows typical set of frames from the high-speed camera obtained from the conducted tests. Frames 5-8 were used to calculate the residual projectile velocity.

A typical case of a threshold impactor velocity (ballistic limit) is shown in Fig. 5. The impactor is almost completely stopped by the target and no penetration is observed, however the target is severely damaged.

Experimental and numerically obtained dependencies of the residual impactor velocity (V_r) on the initial impactor velocity (V_i) are shown in Fig. 6 together with the ballistic limits. The dependencies can be approximated with a straight line for middle range and high impactor velocities, while the V_r values drop abruptly in the near ballistic limit velocity range. Some graphs of the numerical results in Fig. 6 contain negative V_r values, which means that the impactor bounced from the target and no penetration occurred.

The numerical results fit well the experimental data, especially for the thinner plates. In all cases the numerical model could reliably predict the ballistic limit for the studied targets. The $V_r - V_i$ dependence was numerically predicted using the model for a 5mm plate and the ballistic limit for this virtual test configuration was assessed.

Fig. 7 shows both the experimental and numerically evaluated dependencies of the ballistic limit on the specimen thickness together with the numerical prediction for a 5 mm thick plate.

The numerically obtained fracture patterns generally resemble the experimental results. The impact results in crater formation and cracks propagating toward the edges of the sample. For relatively low impactor velocities the fracture pattern is similar. Higher impactor speeds result in shorter cracks comparing to the experimental results. The crack propagation trajectories are defined by the applied boundary conditions – the sample bracing in our case. The fracture patterns for relatively low impact velocities resemble those for the purely quasi-static case – cracks propagating toward the clamps. The fracture pattern changes for the higher impactor velocities, since the effect of the fixation method is less pronounced in this case due to shorter target – projectile interaction time. Relatively short interaction times lead to concentration of the impact energy in the contact spot leading to a more localized fracture. Fig. 8 compares numerical results and experimental fracture patterns for the 10 mm thick plate at three impact velocities including a threshold one (70 m/s).

5. Conclusions

The work contains experimental and numerical results on impact of PMMA plates with various thicknesses using a steel projectile. Dependence between initial impactor velocity V_i and the residual impactor velocity V_r was experimentally assessed using a gas gun and a high-speed photography setup. In addition to this, the ballistic limit for all three sample types was obtained. The experimental data was used to test and validate a numerical approach, which uses the finite element method and the incubation time fracture model for the material failure predictions. The applied scheme is rather simple and involves a limited number of the material parameters. All of the parameters are either standard material data or can be evaluated from the experiments on the PMMA described in the literature (e.g. the incubation time value).

The simulation results appear to be promising: both ballistic limits for the particular targets and the projectile and the $V_r - V_i$ function can be predicted using relatively simple numerical scheme. This way the developed numerical approach can be applied to predict the impact fracture in other cases: for other brittle materials (e.g. ceramics) and other specimen configurations. For example, numerical estimates for the ballistic limit and for the $V_r - V_i$ dependence of the 5 mm thick PMMA plate are presented in the work.

CRediT authorship contribution statement

N.A. Kazarinov: Writing - original draft, Software, Formal analysis. **V.A. Bratov:** Project administration, Conceptualization, Visualization. **N.F. Morozov:** Conceptualization, Funding acquisition. **Y.V. Petrov:**

Methodology, Supervision. **V.V. Balandin:** Investigation, Resources. **M.A. Iqbal:** Project administration, Writing - review & editing, Funding acquisition. **N.K. Gupta:** Conceptualization, Funding acquisition.

Declaration of Competing Interest

The authors declare that they have no known competing financial interests or personal relationships that could have appeared to influence the work reported in this paper.

Acknowledgments

The work was supported by joint grants from Russian Foundation of Basic Research and Department of Science and Technology (India) (grants 16-51-45063/INT/RUS/RFBR/P-232 and 19-51-45016/INT/RUS/RFBR/361). N.A. Kazarinov acknowledges support from Russian Science Foundation (grant 18-71-00107) for creation of chapters 3 and 4.

References

[1] Xu X, Needleman A. Numerical simulations of dynamic crack growth along an interface. Int J Fract 74 1995:289–324. https://doi.org/10.1007/BF00035845.
[2] Liu MB, Liu GR. Smoothed particle hydrodynamics (SPH): an overview and recent developments. Arch Comput Methods Eng 2010;17(1):25–76. https://doi.org/10.1007/s11831-010-9040-7.
[3] Johnson GR. Artificial viscosity effects for SPH impact computations. Int J Impact Eng 1996;18(5):477–88. https://doi.org/10.1016/0734-743X(95)00051-B.
[4] Kosteski LE, Iturrioz I, Cisilino A, D'ambra RB, Pettarin V, Fasce L, Frontini P. A lattice discrete element method to model the falling-weight impact test of PMMA specimens. Int J Impact Eng 2016;87:120–31. https://doi.org/10.1016/j.ijimpeng.2015.06.011.
[5] Belytschko T, Krysl P, Krongauz Y. A three-dimensional explicit element-free Galerkin method. Int J Numer Methods Fluids 1997;24(12):1253–70.
[6] Lee J, Liu W, Hong J-W. Impact fracture analysis enhanced by contact of peridynamic and finite element formulations. Int J Impact Eng 2016;87:108–19. https://doi.org/10.1016/j.ijimpeng.2015.06.012.
[7] Demmie PN, Silling SA. An approach to modeling extreme loading of structures using peridynamics. J Mech Mater Struct 2007;2:1921–45. https://doi.org/10.2140/jomms.2007.2.1921.
[8] Cadoni E, Albertini C, Solomos G. Analysis of the concrete behaviour in tension at high strain-rate by a modified Hopkinson bar in support of impact resistant structural design. J Phys IV France 2006;134:647–52. EURODYMAT 2006 - 8th International Conference on Mechanical and Physical Behaviour of Materials under Dynamic Loading.
[9] Bragov AM, Lomunov AK. Methodological aspects of studying dynamic material properties using the Kolsky method. Int. J. Imp. Eng. 1995;16(2):321–30. https://doi.org/10.1016/0734-743X(95)93939-G.
[10] Ravi-Chandar K. Dynamic fracture of nominally brittle materials. Int. J. Frac. 1998;90:83–102. https://doi.org/10.1023/A:1007432017290.
[11] Fineberg J, Bouchbinder E. Recent developments in dynamic fracture: some perspectives. Int. J Fract. 2015;196:33–57. https://doi.org/10.1007/s10704-015-0038-x.
[12] Grady DE. Fragment size distributions from the dynamic fragmentation of brittle solids. Int J Impact Eng 2008;35:1557–62. https://doi.org/10.1016/j.ijimpeng.2008.07.042.
[13] Johnson G, Cook W. Fracture characteristics of three metals subjected to various strains, strain rates, temperatures and pressures. Eng. Fract. Mech 1985;21(1):31–48. https://doi.org/10.1016/0013-7944(85)90052-9.
[14] Johnson GR, Cook WH. A constitutive model and data for metals subjected to large strains, high strain rates and high. Proceedings of the 7th international symposium on ballistics. 1983. p. 541–7.
[15] Iqbal MA, Senthil K, Bhargava P, Gupta NK. The characterization and ballistic evaluation of mild steel. Int J Impact Eng 2015;78:98–113. https://doi.org/10.1016/j.ijimpeng.2014.12.006.
[16] Allen DJ, Rule WK, Jones SE. Optimizing material strength constants numerically extracted from Taylor impact data. Exp Mech 1997;37(3):333–8. https://doi.org/10.1007/bf02317427.
[17] Irwin G. Analysis of stresses and strains near the end of a crack traversing a plate. J Appl Mech 1957;24:361–4.
[18] Freund LB. Dynamic fracture mechanics. Cambridge: Cambridge University Press; 1990. https://doi.org/10.1017/CBO9780511546761.
[19] Rosakis AJ, Zehnder AT. On the dynamic fracture of structural metals. Int J Fract 1985;27:169–86. https://doi.org/10.1007/BF00017966.
[20] Chung Kim Yuen S, Nurick GN, Langdon GS, Iyer Y. Deformation of thin plates subjected to impulsive load: Part III – an update 25 years on. Int J Impact Eng 2017;107:108–17. https://doi.org/10.1016/j.ijimpeng.2016.06.010.
[21] Zhao YP. Suggestion of a new dimensionless number for dynamic plastic response of beams and plates. Arch Appl Mech 1998;68:524–38. https://doi.org/10.1007/s004190050184.
[22] Petrov YV, Utkin AA. Dependence of the dynamic strength on loading rate. Sov Mater Sci 1989;25(2):153–6https://doi.org/10.1007/BF00780499.
[23] Petrov YV. On "quantum" nature of dynamic failure of brittle media. Dokl Akad Nauk SSSR 1991;321(1):66–8.
[24] Petrov YV, Morozov NF. On the modeling of fracture of brittle solids. J Appl Mech 61 1994:710–2. https://doi.org/10.1115/1.2901518.
[25] Dorogoy AGodinger, Rittel D. Application of the incubation time criterion for dynamic brittle fracture. Int J Impact Eng 2018;112:66–73. https://doi.org/10.1016/j.ijimpeng.2017.09.019.
[26] Fineberg J, Gross SP, Marder M, Swinney HL. Instability in the propagation of fast cracks. Phys Rev B 1992;45(10):5146–54. https://doi.org/10.1103/PhysRevB.45.5146.
[27] Smirnov I, Kazarinov N, Petrov Y. Experimental observation and numerical modelling of unstable behaviour of a fast crack velocity. Theor Appl Fract Mech 2019;101:53–8. https://doi.org/10.1016/j.tafmec.2019.02.006.
[28] Stenzler JS, Goulbourne NC. The effect of polyacrylate microstructure on the impact response of PMMA/PC multi-laminates. Int J Impact Eng 2011;38:567–76. https://doi.org/10.1016/j.ijimpeng.2011.02.003.
[29] Kanel GI. Spall fracture: methodological aspects, mechanisms and governing factors. Int. J. Fract 2010;163:173–91. https://doi.org/10.1007/s10704-009-9438-0.
[30] Parkhomenko IP, Utkin AV, et al. Spall strength of plexiglass. In: Fortoveditor. Investigations of material properties under extremal conditions. Moscow: IVTAN; 1990. p. 126–30. (in Russian).
[31] Rosenberg Z, Surujon Z, Yeshurun Y, Ashuach Y, Dekel E. Ricochet of 0.3'' AP projectile from inclined polymeric plates. Int J Impact Eng 2005;31:221–33. https://doi.org/10.1016/j.ijimpeng.2003.12.008.
[32] Neuber H. Kerbspannunglehre: Grundlagen fur Genaue Spannungsrechnung. Berlin: Springer-Verlag; 1937. https://doi.org/10.1007/978-3-662-36565-6.
[33] Novozhilov VV. About the necessary and sufficient brittle strength criterion. Prikl. Mat. Mekh 1969;33(2):212–22. https://doi.org/10.1016/0021-8928(69)90025-2.
[34] Petrov YuV, Gruzdkov AA, Bratov VA. Structural-temporal theory of fracture as a multiscale process. Phys Mesomech 2012;15(3-4):232–7. https://doi.org/10.1134/S1029959912020117.
[35] Varela-Rizo H, Weisenberger M, Bortz DR, Martin-Gullon I. Fracture toughness and creep performance of PMMA composites containing micro and nanosized carbon filaments. Composites Sci Technol 2010;70:1189–95. https://doi.org/10.1016/j.compscitech.2010.03.005.
[36] Kazarinov NA, Bratov VA, Petrov YV. Simulation of dynamic crack propagation under quasi-static loading. Doklady Phys 2014;59(2):99–102. https://doi.org/10.1134/S1028335814020116.